Rock Mech Rock Eng (2010) 43:657–666
DOI 10.1007/s00603-010-0091-8

ORIGINAL PAPER

Some Fundamental Issues in Dynamic Compression and Tension Tests of Rocks Using Split Hopkinson Pressure Bar

Feng Dai · Sheng Huang · Kaiwen Xia · Zhuoying Tan

Received: 10 December 2009 / Accepted: 2 March 2010 / Published online: 16 March 2010

Abstract Accurate characterizations of rock strengths under higher loading rates are crucial in many rock engineering applications. The split Hopkinson pressure bar (SHPB) system has been used to quantify the dynamic compressive strength of rocks using the short cylindrical specimen and the dynamic tensile strength of rocks using the Brazilian disc (BD) specimen. However, SHPB is a standard tool that is suitable for metal testing; there are some fundamental issues that need to be carefully visited in applying SHPB to rock dynamic tests. This paper addresses several such critical issues, including the choice of slenderness ratio of the compressive specimen, the effect of friction between the sample and bars on the measured results of compressive strength, the necessity of dynamic force balance on the dynamic BD test, and the validity of using the standard BD equation in the data reduction. We show that with proper experimental designs that address these issues, the dynamic compressive strength and dynamic tensile strength of rocks measured using SHPB are valid and reliable.

Keywords SHPB · Friction effect · Slenderness ratio · Dynamic force/stress balance

F. Dai · S. Huang · K. Xia (✉) · Z. Tan
Department of Civil Engineering, Lassonde Institute, University of Toronto, Toronto, ON M5S 1A4, Canada
e-mail: kaiwen.xia@utoronto.ca

F. Dai
State Key Laboratory of Geomechanics and Geotechnical Engineering, Institute of Rock and Soil Mechanics, Chinese Academy of Sciences, 430071 Wuhan, People's Republic of China

1 Introduction

In many mining and civil engineering applications, such as quarrying, rock cutting, drilling, tunnelling, rock blasts, and rock bursts, rocks are loaded and/or failed dynamically. Accurate characterizations of rock strength properties under higher loading rates are thus crucial. The split Hopkinson pressure bar (SHPB) system developed by Kolsky (1949, 1953) has been widely used to investigate the dynamic compressive responses of engineering materials at high strain rates in the range of 10^2–10^4 s^{-1} (Gray 2000). SHPB has been introduced to dynamic rock tests in dynamic compressive tests (Cai et al. 2007; Li et al. 2000; Olsson 1991) and dynamic tensile strength with Brazilian disc (BD) sample geometry (Cai et al. 2007; Wang et al. 2006). However, there are several critical issues remaining to be addressed to ensure that the values of dynamic rock strengths are valid and reliable. These issues are the effect of friction between the sample and bars on the compressive strength of rocks, the choice of slenderness ratio of the compressive specimen, the necessity of dynamic force balance for the dynamic BD test, and the validity of using the standard BD equation in the data reduction in dynamic tests.

The compressive tests of SHPB are based on two fundamental assumptions: (1) one-dimensional (1D) elastic wave propagation in the bars and (2) homogeneous deformation of the sample (Kolsky 1953). The assumption of 1D stress wave propagation is ensured by using long bars, and the elasticity of the bar deformation is guaranteed throughout the test by limiting the impacting velocity of the striker. The homogeneity of the sample deformation is affected mainly by two factors: inertial effects (i.e., the axial inertial effect and the radial inertial effect) and the interfacial friction effect.

The ideal slenderness ratio (i.e., the length to diameter ratio) of the sample has long been studied because it plays a major role on the inertial effects during the dynamic SHPB test. Based on the synthetic analysis of both axial and radial inertia effects, Davies and Hunter (1963) suggested an optimal slenderness ratio of $L/D = \sqrt{3}v/2$, where L and D are the length and diameter of the cylindrical sample, respectively, and v is the Poisson's ratio of the testing material. This suggested slenderness ratio has been frequently used to design the sample geometry for metals (Meng and Li 2003). To limit the inertia effects associated with stress wave loading, the slenderness ratio of samples cannot be too large. When SHPB is first introduced to the dynamic testing community, the incident wave is in rectangular shape with a sharp rising edge and highly oscillation, it is harder to minimize the axial inertial effects because it takes longer time for the sample to reach stress equilibrium. However, with recent developed pulse shaping technique (Frew et al. 2001, 2002), even a relative long compressive sample can easily obtain stress equilibrium, thus reducing the axial inertial effects to a negligible amount. In this case, the suggested ratio of $L/D = \sqrt{3}v/2$ by Davies and Hunter (1963) is too conservative under current vision with pulse shaping technique. For example, the L/D ratio for an incompressible material (with v equal to 0.5) is determined to be 0.433. As will be discussed later, for short samples like this, friction at boundary can markedly affect the inner stress state, and thus the homogeneity of the sample deformation.

Friction effect is another major concern in the SHPB test. As early as SHPB was first introduced as a useful dynamic testing tool, it was realized that the interfacial friction on both ends of the sample may affect the testing results (Kolsky 1949, 1953). When the sample is loaded by the compressive stress wave in the SHPB test, it expands radially due to the Poisson's effect. If the sample/bar interfaces are not sufficiently lubricated, the resulting interfacial friction force can be significant. This friction force influences the accuracy of the testing results by applying a dynamic confinement to the compressive specimen, whose stress state should be 1D stress by assumption. This additional stress can yield pseudo rate effects of the sample material (Schey et al. 1982). For example, Hauser et al. (1960) mistakenly concluded that the aluminium alloy was a rate sensitive material because they glued the sample on the bars during their tests. In addition, the sample is no longer deformed uniformly because of this dynamic confinement (Narayanasamy and Pandey 1997), whose effect is the largest on the ends and diminishes towards the centre of the specimen. Bell (1966) examined the distribution of stress and strain in the SHPB tests and found that there exists marked discrepancy between the measured strain from SHPB data reduction and the strain directly measured from the sample surface. With finite difference method, Bertholf and Karnes (1975) simulated SHPB tests on samples with three types of slenderness ratios and interfacial frictions to investigate both inertial effects and interface friction effects. They drew the same conclusion as Bell (1966) that without enough lubrication at the boundary interfaces, the stress state in the sample is inhomogeneous and big deviation of measurement occurs inevitably. Malinowski and Klepaczko (1986) presented a united analytic and numerical approach to investigate inertia and friction effects in SHPB tests on annealed aluminium through the consideration of energy balance. They concluded that proper treatment of frictional effects, along with inertia is crucial for an exact determination of the material response during plastic deformation. Meng and Li (2003) recently revisited the combined effects of slenderness ratio and the interface friction numerically. To limit the frictional effect, the slenderness ratio of a compressive sample should be large enough. This can be manifested from a recommended slenderness ratio of 2 or larger for static compressive tests of rocks by International Society for Rock Mechanics (ISRM) (Bieniawski and Bernede 1979). On the other hand, the slenderness ratio should be short enough to limit the inertia effects. Thus, an optimal slenderness ratio is needed to address both the inertial effects and the friction effect.

SHPB has also been adopted to conduct indirect tension tests for measuring the tensile strength of brittle solids like rocks. For examples, conventional SHPB tests were conducted using BD method on marbles (Wang et al. 2006) and argillites (Cai et al. 2007). These attempts followed the pioneer work on dynamic BD tests of concretes using SHPB (Ross et al. 1989, 1995). Semi-circular bending samples were used also in SHPB to measure the flexural tensile strength of Laurentian granite (LG) (Dai et al. 2009). BD method has been suggested by ISRM as a recommended method for tensile strength measurement of rocks (Bieniawski and Hawkes 1978). Using BD method, Zhao and Li (2000) measured the dynamic tensile properties of granite using a hydraulic loading system. For quasi-static and low speed BD tests, it is reasonable to use the standard static equation to calculate the tensile strength. However, for dynamic BD test conducted with SHPB featuring stress wave loading, the application of the quasi-static equation to the data reduction has not yet been rigorously checked (Cai et al. 2007; Wang et al. 2006). In this work, we will investigate the conditions under which the static analysis is valid.

The texts are organized as follows. In Sect. 2, the experimental setup of SHPB system and the testing methodologies are presented. Section 3 manifests the friction effects considering three different contact conditions of the bar and the sample: lubricated contact, dry contact and bonded contact. In addition, the dynamic compressive

strengths are measured for samples with slenderness ratios ranging from 0.5 to 2.0. In Sect. 4, dynamic BD tests are conducted with two different loading conditions: without pulse shaping, and with careful pulse shaping and thus dynamic force balance. With the aid of high speed camera, the failure sequences of the disc samples are visualized. The validation of the quasi-static tensile strength reduction is assessed for both cases. Conclusions are drawn in Sect. 5.

2 Experimental Setup and Methodologies

2.1 The Split Hopkinson Pressure Bar System

A 25 mm in diameter SHPB system is used in this research, which is composed of a striker bar (200 mm in length), an incident bar (1,500 mm in length) and a transmitted bar (1,200 mm in length), all made of high strength maraging steel (Fig. 1a). The specimen is sandwiched between the incident and transmitted bars. Two strain gauges are mounted on the incident bar and transmission bar, respectively. During the tests, the impact of a striker bar on the free end of the incident bar induces a longitudinal compressive wave (incident wave) propagating in the incident bar. When the compressive incident wave reaches the bar-specimen interface, it is partly reflected (reflected wave), and the remainder passes through the specimen to the transmitted bar (transmitted wave). These three elastic stress pulses in the incident and transmitted bars are recorded with the strain gauges and denoted as the input strain pulse $\varepsilon_i(t)$, reflected strain pulse $\varepsilon_r(t)$and transmitted strain pulse $\varepsilon_t(t)$, respectively.

2.2 Standard Analysis of SHPB

Based on 1D stress wave theory (Kolsky 1953), the dynamic forces on the incident end (P_1) and the transmitted end (P_2) of the specimen are:

$$P_1 = AE(\varepsilon_i + \varepsilon_r), \quad P_2 = AE\varepsilon_t \tag{1}$$

The displacement of the incident bar end (u_1) and the transmitted bar end (u_2) are:

$$u_i = C\int_0^t (\varepsilon_i - \varepsilon_r)\mathrm{d}t, \quad u_2 = C\int_0^t \varepsilon_t \mathrm{d}t \tag{2}$$

In the above equations, E is the Young's Modulus of the bar, A the area of the bar, and C is the 1D longitudinal

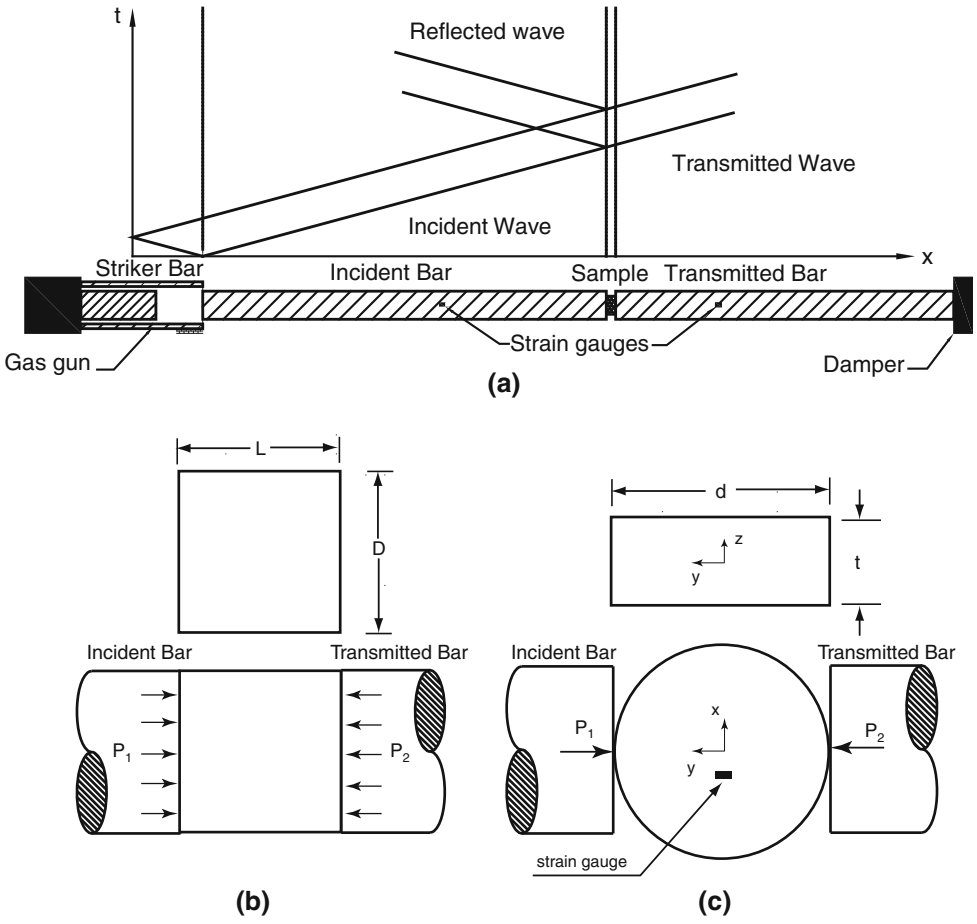

Fig. 1 **a** Schematics of a split Hopkinson pressure bar (*SHPB*) system and the *x–t* diagram of stress waves propagation in SHPB, **b** close-view of the compression test and **c** close-view of the tension test (Brazilian test) with SHPB

stress wave velocity of the bar. The histories of strain rate $\dot{\varepsilon}(t)$, strain $\varepsilon(t)$ and stress $\sigma(t)$ within the sample in the dynamic compression tests (Fig. 1b) can be calculated as (Gray 2000):

$$\begin{cases} \dot{\varepsilon}(t) = \dfrac{C}{L}(\varepsilon_i - \varepsilon_r - \varepsilon_t) \\ \varepsilon(t) = \dfrac{C}{L}\displaystyle\int_0^t (\varepsilon_i - \varepsilon_r - \varepsilon_t)\mathrm{d}t \\ \sigma(t) = \dfrac{A}{2A_0}E(\varepsilon_i + \varepsilon_r + \varepsilon_t) \end{cases} \tag{3}$$

where L is the length of the sample and A_0 is the initial area of the sample. Assuming the stress equilibrium prevails during dynamic loading (i.e., $\varepsilon_i + \varepsilon_r = \varepsilon_t$), the commonly used formulas are obtained:

$$\begin{cases} \dot{\varepsilon}(t) = -\frac{2C}{L}\varepsilon_r \\ \varepsilon(t) = -\frac{2C}{L}\displaystyle\int_0^t \varepsilon_r \mathrm{d}t \\ \sigma(t) = \frac{A}{A_0}E\varepsilon_t \end{cases} \tag{4}$$

2.3 Dynamic BD Tests with SHPB

A close-view of the dynamic BD test in the SHPB system is schematically shown in Fig. 1c, where the disc sample is sandwiched between the incident bar and the transmitted bar. The principle of BD test comes from the fact that rocks are much weaker in tension than in compression and thus the diametrically loaded rock disc sample fails due to the tension along the loading diameter near the centre. The calculation equation of tensile strength is based on the two-dimensional (2D) elastic analysis as (Michell 1900):

$$\sigma_{\mathrm{t}} = \frac{2P_{\mathrm{f}}}{\pi dt} \tag{5}$$

where P_{f} is the load when the failure occurs, σ_{t} is the tensile strength, d and t are the diameter and the thickness of the disc, respectively.

A strain gauge is glued on the disc surface with 5 mm away from the centre of the disc (Fig. 1c). The cracking of the disc centre emits elastic release waves upon cracking, and this wave causes sudden strain drop in the recorded strain gauge signal (Jiang et al. 2004). The peak point of the strain gauge signal right before the sudden drop corresponds to the arrival of the release wave due to crack initiation. It is noted that the original strain gauge signal should be corrected accordingly considering the time the elastic wave propagates from disc centre to the strain gauge.

2.4 Sample Preparation

An isotropic fine-grained granitic rock, LG is chosen for this research, whose mineralogical and mechanical characteristics are well documented (Nasseri et al. 2005). LG is taken from the Laurentian region of Grenville province of the Precambrian Canadian Shield, north of St. Lawrence and north-west of Quebec City, Canada. The mineral grain size of LG varies from 0.2 to 2 mm with the average quartz grain size of 0.5 mm and the average feldspar grain size of 0.4 mm, with feldspar being the dominant mineral (60%) followed by quartz (33%). Biotite grain size is of the order of 0.3 mm and constitutes 3–5% of this rock. Rock cores with nominal diameters of 25 and 40 mm are first drilled from the rock blocks. For the 25 mm in diameter cores, we directly slice them to obtain cylindrical samples with varying slenderness ratios (i.e., L/D, see Fig. 1b) from 0.5, 1.0, 1.5 to 2.0. Those cylindrical samples are prepared for dynamic compressive tests. For the dynamic BD test, we slice the 40 mm in diameter core into discs with nominal thickness of 20 mm. All the disc samples are polished afterwards resulting in surface roughness of <0.5% of the sample thickness. It is noted here that the dimension of the samples are ten times larger than the grain size, which is consistent to the ISRM standards for static UCS and BD tests. For coarse-grain rocks, larger diameter samples are needed and thus larger diameter SHPB systems are needed. The conclusions in this work are valid for SHPB system regardless of the bar diameter.

3 SHPB Compressive Tests

3.1 Slenderness Ratio

The slenderness ratio has been a fundamental issue in the dynamic compression test with SHPB because it has a major influence on the axial inertia effects of the sample. The higher the slenderness ratio of a sample, the higher the axial inertial effects and the lower the relative radial inertial effects involved; and vice versa. In the conventional SHPB test, a rectangular incident wave is generated by a direct impact of the striker to the free end of the incident bar. This incident wave features a very sharp arising part as well as great oscillations; and it takes longer time for the sample to reach dynamic stress equilibrium. For brittle solids like rocks with small failure strain, the sample may fail immediately from its end when it is impacted by the incident bar.

Recently, pulse shaping technique has been widely utilized for SHPB testing on engineering materials and it is especially useful for investigating dynamic response of brittle materials such as rocks (Frew et al. 2001, 2002). During tests, the striker impacts the pulse shapers right before the incident bar, generating a non-dispersive ramp pulse propagating into the incident bar and thus facilitating

the dynamic stress equilibrium in the specimen (Frew et al. 2001, 2002). Under stress equilibrium, the stress gradient vanishes, and inertial effects induced by stress wave propagation are thus minimized. In the modified SHPB test, we use the C11000 copper disc in combination with a small rubber disc together as the shaper to transform the incident wave from a rectangular shape to a ramped shape (Xia et al. 2008). Figure 2 shows the dynamic stresses in a typical compressive test. Based on the 1D stress wave theory, the time zeros of the incident and reflection stress waves in Fig. 2 are shifted to the sample-incident bar interface and the sample-transmitted bar interface, respectively. From Eq. 3, the dynamic force on one side of the specimen P_1 is the sum of the incident and reflected waves (In. + Re.), and the dynamic force on the other side of the specimen P_2 is the transmitted wave (Tr.). It is shown that the time-varying stresses on both sides of the samples match with each other before the peak point is reached during the dynamic loading. The sample is thus in a state of dynamic stress equilibrium. It is also noted that the resulting stress on either side of the sample also feature a linear portion before the peak, thus facilitating a constant loading rate via $\sigma = k_1 A/A_0$. The parameter k_1 in the equation is illustrated in Fig. 2.

We conducted compressive tests on cylindrical rock samples with varying slenderness ratio from 0.5, 1.0, 1.5 to 2.0. For all tests, we achieved dynamic stress equilibrium. Since there is no stress gradient in the sample, the axial inertial effect is thus negligible. In addition, to minimize the disturbance from the boundary frictions on the measured strength, the bar/sample interfaces for all samples are fully lubricated with vacuum grease. The measured compressive strengths with corresponding loading rates are shown in Fig. 3. There are no significant differences of

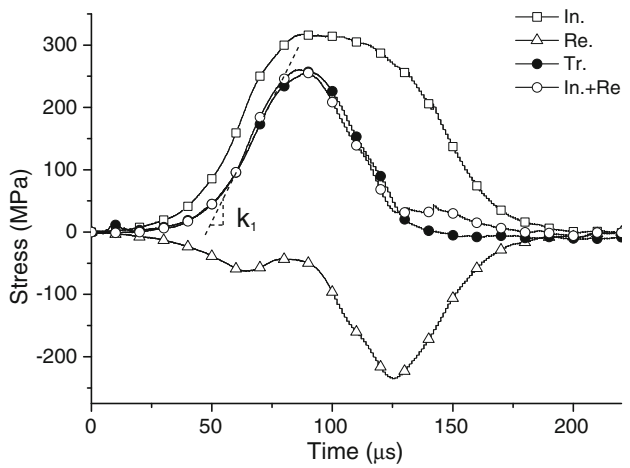

Fig. 2 Dynamic stresses on both ends of disc specimen tested using a modified SHPB with careful pulse shaping

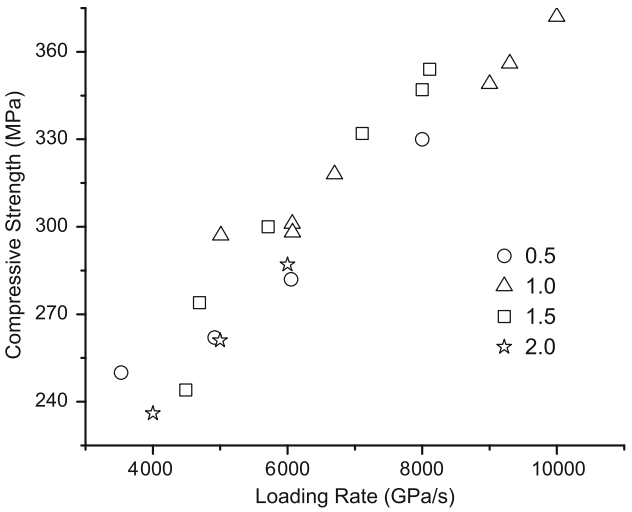

Fig. 3 Dynamic compressive strengths with loading rates measured from rock samples with varying slenderness ratio of 0.5, 1.0, 1.5 and 2.0

strengths from samples with selected slenderness ratios. For dynamic compressive tests on rocks, we conclude that with bar/sample interfaces fully lubricated and thus with axial inertial effects minimized, the slenderness ratio has little influences on the testing results within the range of 0.5–2. Samples with $L/D < 0.5$ are very hard to fabricate because it is difficult to hold the sample during cutting and polishing processes. In addition, shorter samplers suffer worse fabrication damage problems. On the other hand, for long samples like $L/D = 2$, very high driving force is needed to achieve high loading rates, that is why data with strain rate higher than 6×10^3 for $L/D = 2$ are missing because otherwise the bars may be yield or bended. Considering the trade-off, we think $L/D = 1$ is a reasonable choice of sample slenderness ratio for SHPB tests. We thus suggest using samples with a slenderness ratio of 1.0 in dynamic compressive tests of rocks for convenience. The static uniaxial compressive strength of LG is about 220 MPa based on the data measured with the ASTM Standard C170-90 (1999) as published on the website of Rock of Ages Corporation, which is much less than the dynamic compressive strengths measured with our SHPB tests.

3.2 Friction Effect

To manifest the friction effect, we conducted tests on samples (slenderness ratio = 1.0) with three different friction boundaries on the bar/sample interfaces: lubricated, dry and bonded. High strength adhesive is used to bond the sample surfaces to the bar interfaces. The bonded bar–sample interface completely restricts the motion of the rock surfaces on the bar and is believed to provide the maximum

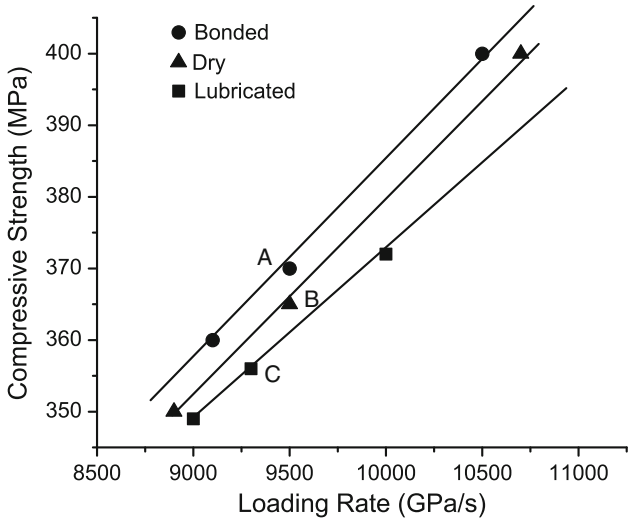

Fig. 4 Dynamic compressive strengths with loading rates measured from rock samples ($L/D = 1.0$) with three interfacial friction boundaries

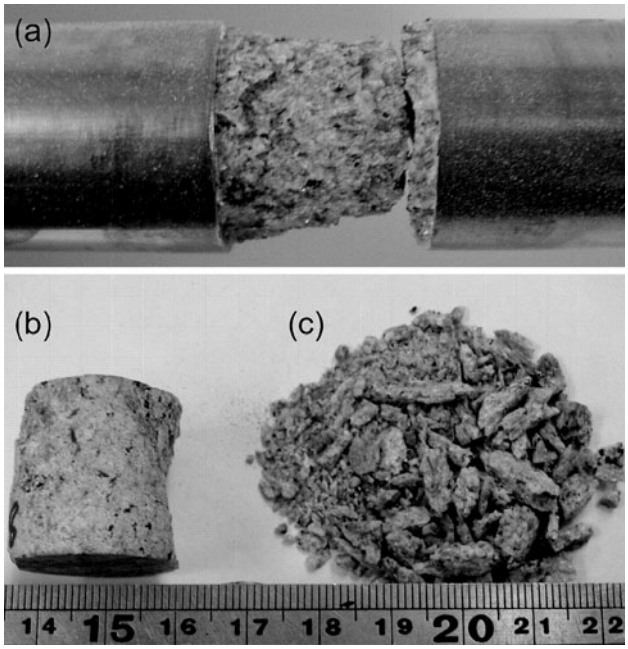

Fig. 5 Photograph of recovered samples with **a** bonded, **b** dry, **c** lubricated bar/sample interfaces showing the damaged level

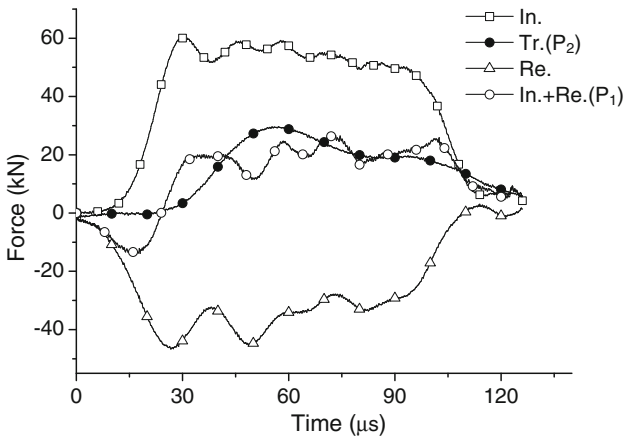

Fig. 6 Dynamic forces on both ends of the disc specimen tested using a traditional SHPB without pulse shaping

dynamic confinement to the sample. Through proper pulse shaping, we guarantee the dynamic stress balance on both ends of the sample (Fig. 2) and a constant loading rate has been achieved for all tests. Figure 4 illustrates the trend of the rate effects of compressive strength under these three boundary friction conditions. Samples with bar/samples interfaces fully lubricated yield the lowest measured compressive strength while the samples with bonded interfaces own the highest. The friction effect in dynamic compressive tests on rocks is significant. The measured compressive strength increases with increasing friction involved in the tests. To obtain the actual dynamic compressive response of rocks, the bar–sample interfaces should be sufficiently lubricated.

Figure 5 shows the recovered samples with (a) bonded (b) dry (c) lubricated bar/sample interfaces, coming from the tests with the data points of A, B and C in Fig. 4, respectively. For these three typical tests, we load the sample with approximately the same incident wave; however, the damage levels of them are quite different. With bar/sample interfaces fully lubricated, the samples are completely fragmented into small pieces (Fig. 5c), featuring a typical splitting failure mode. In contrast, with friction constrain at the boundary interfaces, the splitting is constrained significantly and the recovered samples feature a shear cone as shown in Fig. 5a, b. With approximated similar loading rates, the strength (at point A) of the sample with bonded interfaces (i.e., with the maximum induced friction) is the maximum (Fig. 4); while fully lubricated sample yields the lowest strength (at point C). The sample with dry friction interfaces has an intermediate strength level (at point B).

4 Dynamic BD Tests using SHPB

4.1 Dynamic BD Tests Without Pulse Shaping

4.1.1 Dynamic Forces and Failure Sequences with High Speed Camera

Traditionally, by the direct impact of the striker on the free end of the incident bar in a SHPB test, the generated incident wave is a square compressive stress wave with a very sharp arising portion, which inevitably introduces high frequency oscillations. As a result, the dynamic forces on both ends of the sample vary significantly. Evidently, Fig. 6

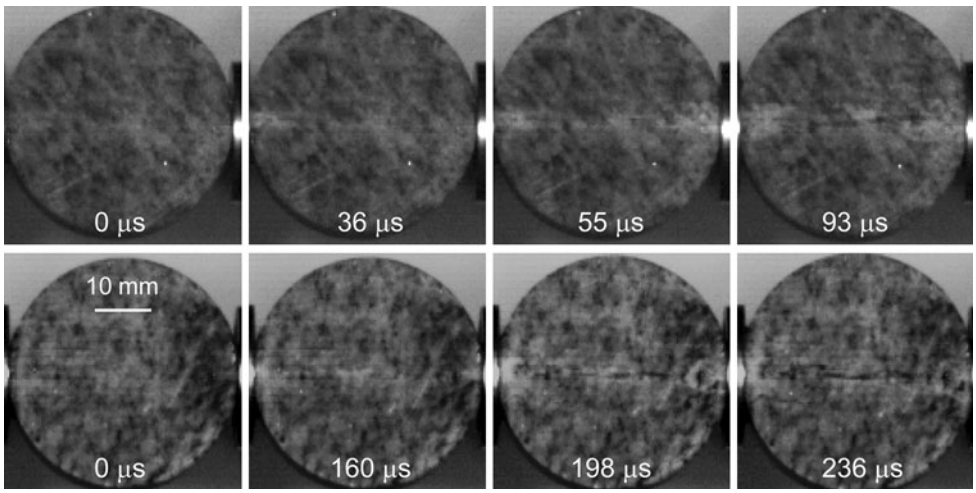

Fig. 7 High-speed video images of two typical dynamic Brazilian tests; *top* four images: Brazilian test without pulse shaping; *bottom* four images: Brazilian test with careful pulse shaping

depicts a large oscillation of dynamic force occurring on the incident side and a sizeable distinction between P_1 and P_2.

4.1.2 Failure Sequences with High Speed Camera

For a valid Brazilian test, the disc sample should break first along the loading direction somewhere near the centre of the disc. To verify this, we used a Photron Fastcam SA5 high speed camera to monitor the fracture processes of the BD test without pulse shaping. The high speed camera is placed perpendicular to the sample surface with images taken at an inter frame interval of 3.8 μs. The failure process of this test without shaping the loading incident wave has been shown as top four images of Fig. 7. The time zero corresponds to the moment when the incident pulse arrives at incident bar–sample interface. We observe the first breakage emanates from the incident size of the sample at around 36 μs after the incident wave arrives at the bar/sample interface. Soon after that, damages also occur from the transmitted side of the sample (see the image at 55 μs). Thus, the splitting of the disc (see, the image at 93 μs) is triggered by the damages at the loading points and then expands to the centre of the disc. We thus conclude that in this case, the working principle of a BD test is violated. The rectangular incident loading wave with a sharp rising edge (Fig. 6) seems to affect the failure mode of the testing sample significantly. Since the cracking of the BD initiates from the loading ends, not from somewhere near the centre of the disc, the standard equation (Eq. 5) is invalid for reducing the tensile strength from the tensile stress history at the disc centre.

4.2 Dynamic BD Tests with Careful Pulse Shaping

4.2.1 Dynamic Forces and Failure Sequences with High Speed Camera

As a typical example of SHPB Brazilian tests, Fig. 8 illustrates the time-varying forces in a typical test with

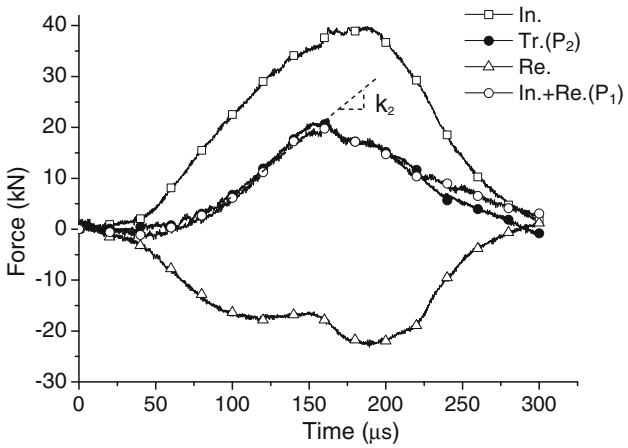

Fig. 8 Dynamic forces on both ends of disc specimen tested using a modified SHPB with careful pulse shaping

careful pulse shaping. The incident wave is shaped to a ramp pulse with a rising time of 180 μs, and a total pulse width of 300 μs. It is evident that the time-varying forces on both sides of the samples are almost identical before the peak point is reached during the dynamic loading. The resulting forces on either side of the sample also feature a linear portion before the peak, thus facilitating a constant loading rate via $\dot{\sigma} = 2k_2/(\pi dt)$, where the parameter k_2 is illustrated in Fig. 8.

High speed camera has also been accommodated to capture the failure sequences of the BD sample with force balance achieved in the test. Bottom four images of Fig. 7 presents the key frames with representative features. In sharp contrast to the images from the non-pulse-shaped BD tests, this disc cracks near the centre and the primary crack occurs at around 160 μs, then propagates bilaterally to the loading ends. The next two frames illustrate the splitting trajectory of the sample; and the disc specimen is split completely into two fragments approximately along the centre line of the sample (Fig. 7). We also note that after

the initiation of the primary crack, one secondary crack is visible near the loading ends at time instant 236 μs. Thus, since the splitting of the disc initiates near the centre, not from the loading ends, the tensile strength can be determined as long as we can accurately determine the tensile stress of the disc at failure. Next, we need to evaluate whether the standard BD equation (Eq. 5) can be used to reduce the tensile strength.

4.2.2 Validation of Quasi-Static BD Equation

For a conventional dynamic compression tests with SHPB or direct tension tests with split Hopkinson tension bar (SHTB), the samples are cylindrical and thus the force balance on the ends ensures the stress equilibrium throughout the sample. However, the disc is 2D; force balance on the boundaries (Fig. 8) does not necessarily ensure dynamic equilibrium within the entire sample. A further compare of the stress history at a point of interest from full dynamic analysis with that from quasi-static analysis is necessary. The dynamic finite element analysis represents the accurate stress history. A commercial finite element software ANSYS is employed in the calculation. The finite element model is meshed with quadrilateral eight-node element PLANE82, with total 4,800 elements and 14,561 nodes (Fig. 9).

Assuming linear elasticity, this analysis solves the following equation of motion with the Newmark time integration technique:

$$\nabla \cdot \sigma = \rho \ddot{u}, \tag{6}$$

where σ is the stress tensor, ρ denotes density, and $\ddot{u}$ is the second time derivative of the displacement vector. The input loads in the finite element model are taken as the dynamic loading forces exerted on the incident and transmitted side of the specimen calculated using Eq. 1 with measured waves.

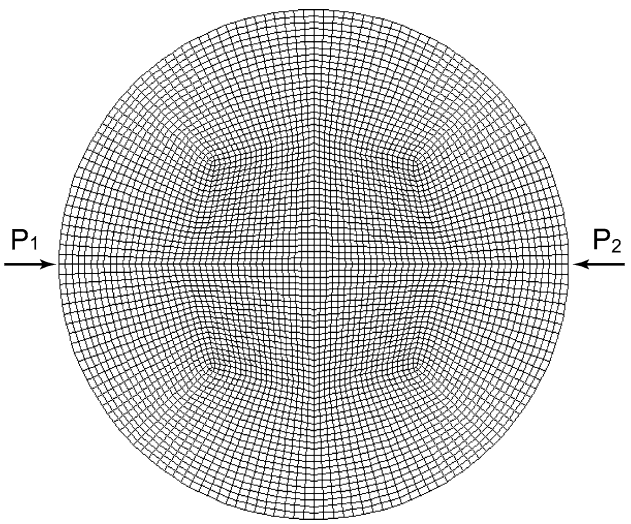

Fig. 9 Mesh of the disc for the finite element analysis

The transient dynamic stress history at the disc centre (potential failure spot) is calculated and compared with that from a quasi-static analysis employing Eq. 5. The histories of the stress components σ_x (in tension) and σ_y (in compression) for dynamic and quasi-static finite element analyses are compared in Fig. 10a, b, respectively. The stress states at the disc centre from both quasi-static and dynamic data reductions match with each other. Thus, provided force balance on the sample ends, the quasi-static analysis with the far-field loading measured as input can accurately represent the stress history in the sample.

Figure 11 shows the signal of the strain gauge mounted on the sample, compared with the transmitted force. Only one peak (A) of the signal is registered by the stain gauge, occurring at time 149 μs. Thus, the breakage initiation time is designated by the unique trough A at the time of 149 μs. Because the peak transmitted force occurs at time 152.5 μs, it is thus delayed only by 3.5 μs after the measured onset of

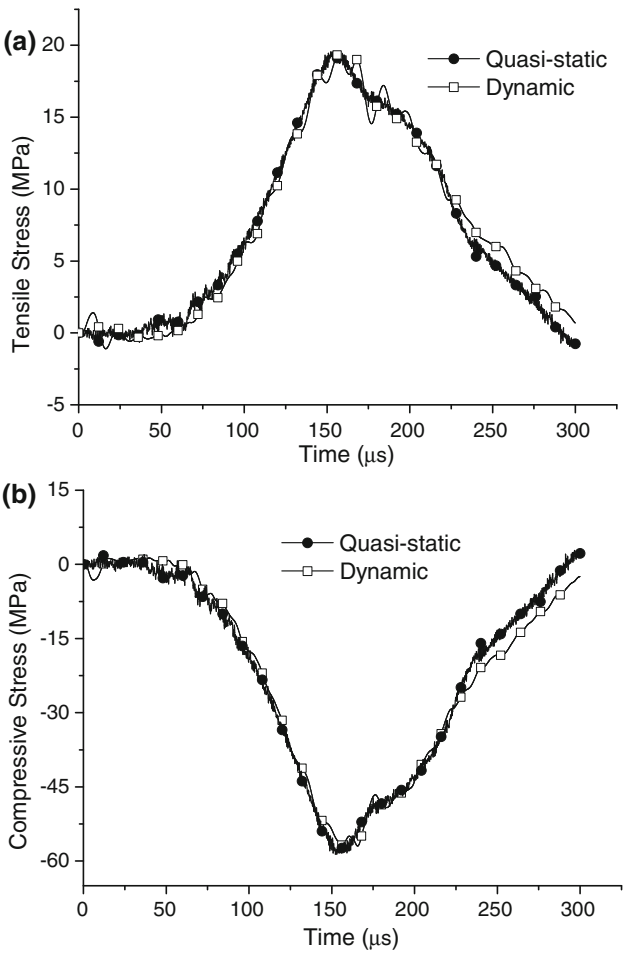

Fig. 10 **a** Tensile stress σ_x, **b** compressive stress σ_y histories at the Brazilian disc centre from both dynamic and quasi-static finite element analyses in a typical SHPB Brazilian test with pulse shaping

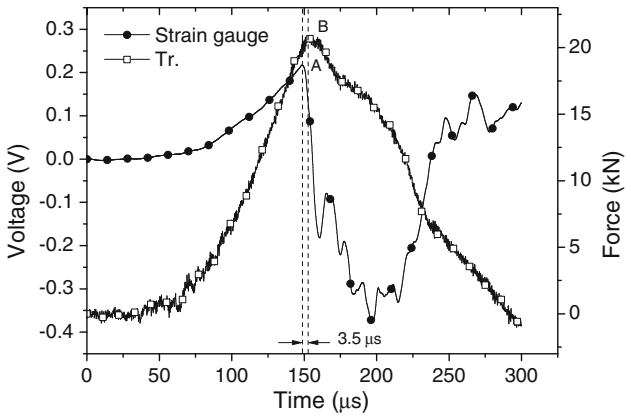

Fig. 11 Comparison of the strain gage signal with the transmitted force for a dynamic Brazilian test using a modified SHPB with careful pulse shaping

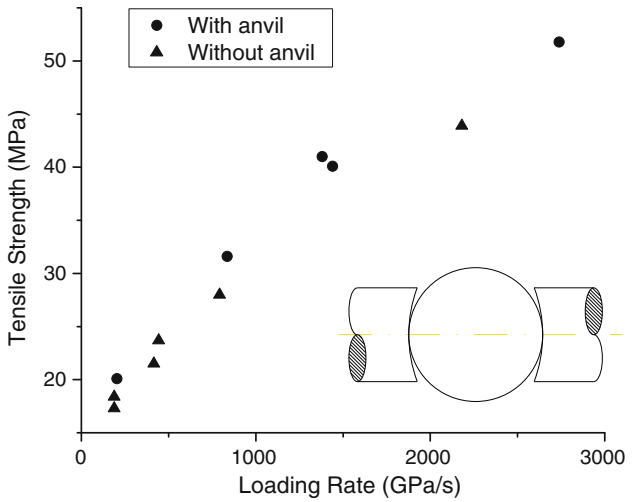

Fig. 12 The measured tensile strength of LG from dynamic Brazilian tests with and without employing jaws

breakage. We conclude that in this case, the peak far-field load matches with the breakage onset with negligibly small time difference. The small time difference of 3.5 μs can be interpreted as follows. The release waves travel at the sound speed of the rock material (around 5 km/s) and the distance between the fracture location and the supporting pin is 20 mm. It thus takes around 4 μs for the first release wave to reach the supporting pins, where the transmitted wave is recorded and also illustrated in Fig. 11. Due to the interaction between the release wave and the pins, the load on the transmitted side decreases (Fig. 11). Thus, the peak of the transmitted force can be regarded as synchronous with the single peak of the strain gauge signal (the rupture onset).

From Figs. 10 and 11, we can conclude that, provided force balance has been achieved on both ends of the BD, the dynamic tensile strength can be reduced from the quasi-static equation (Eq. 5). For the particular test shown above, the measured tensile strength in the SHPB Brazilian test with proper pulse shaping is calculated to be 18.9 MPa at a loading rate of 233 GPa/s.

4.2.3 Necessity of Using the Loading Jaws in Dynamic BD Tests

It is noted that in the ISRM suggested Brazilian test method, two steel loading jaws are used to transfer the load to the disc shaped rock samples diametrically over an arc angle of approximately 10° at failure (Bieniawski and Bernede 1979). The jaws are designed to reduce the localized stress concentration at the loading ends and thus to prevent pre-mature failure. This technique works well for static loading while for SHPB tests, the extra interfaces between the bar and the jaw will complicate the wave stress propagation and increase the difficulties of experimentation. Furthermore, in the foregoing high speed camera snapshots of the dynamic Brazilian test without jaws, no obvious pre-mature breakages are observed. We thus conclude that for SHPB tests, the loading jaws might not be necessary. To further assess this postulation, we conducted two sets of dynamic BD tests, one with jaws and one without jaws. These tests were conducted with careful pulse shaping and thus the dynamic force balance was achieved in all tests.

The radius of the jaws is chosen as 30 mm, 1.5 times of the radius of the disc sample as suggested by the ISRM standard (Bieniawski and Bernede 1979). Figure 12 illustrates the measured tensile strength of LG from dynamic Brazilian tests with and without employing curved jaws at the loading ends; the insert in Fig. 12 shows the sample assembly with the loading jaws. The consistency of the strength values from two sets of tests clearly confirmed our assumption. The simplicity of the experimentation will facilitate the standardization of the dynamic BD method using SHPB.

5 Conclusions

In this paper, we address several fundamental issues in the dynamic compression and tension tests (i.e., Brazilian tests) of rocks with SHPB. For compression tests, we examined the shape effect (length to diameter ratio) and the friction effect during SHPB tests. Cylindrical rock samples with varying length to diameter ratios from 0.5 to 2 are tested. With dynamic stress equilibrium achieved in the samples, the axial inertia effect is tremendously minimized; the influence of the slenderness ratios on the measured strength is negligible. In addition, three different contact cases of the bar/sample: lubricated interface, dry interface and bonded interface are considered and the measured strengths are shown to increase with increasing

friction in the tests. To obtain the actual dynamic compressive response of rocks, the bar–sample interfaces should be fully lubricated. With proper lubrication, we suggest a sample slenderness ratio of 1.0 for dynamic compressive tests of rocks using SHPB.

For dynamic BD tests, we observed that in a pulse shaped SHPB test, the splitting of the disc starts approximately from the centre with the aid of a high speed camera. This is not the case for tests without pulse shaping. We then further examined the usage of static analysis of dynamic BD tests given dynamic force balance. We demonstrate that with dynamic force balance achieved by the pulse shaping technique, the peak of the far-field load synchronizes with the fracture time of the crack gauge at the disc centre and the time-varying dynamic forces on both ends of the sample are almost identical. Furthermore, the evolutions of dynamic compressive stress and tensile stress at the centre of the disc obtained from the dynamic finite element analysis agree with those from quasi-static analysis. These results fully prove that with dynamic force balance in SHPB, the inertial effect is minimized for samples with complex geometries like BD. The dynamic force balance thus enables the regression of tensile strength from dynamic Brazilian test using quasi-static analysis. In addition, we showed that the loading jaw design in the static BD tests can be eliminated in the dynamic BD tests without decreasing the measurement accuracy. To conclude, the dynamic compressive strength and dynamic tensile strength of rocks measured using SHPB are reliable with careful experimental implementations.

Acknowledgments The authors acknowledge the support by NSERC/Discovery Grant No. 72031326 and the CAS/SAFEA International Partnership Program for Creative Research Teams. The authors are grateful to Professor Giovanni Barla and two anonymous reviewers for their constructive comments and valuable time devoted to improving our manuscript.

References

ASTM Standard C170-90 (1999) Standard test method for compressive strength of dimension stone. ASTM International, USA

Bell JF (1966) An experimental diffraction grating study of the quasi-static hypothesis of the split Hopkinson bar experiment. J Mech Phys Solids 14(6):309–327

Bertholf LD, Karnes CH (1975) Two dimensional analysis of the SHPB system. J Mech Phys Solids 23:1–19

Bieniawski ZT, Bernede MJ (1979) Suggested methods for determining the uniaxial compressive strength and deformability of rock materials. Int J Rock Mech Min 16(2):137–138

Bieniawski ZT, Hawkes I (1978) Suggested methods for determining tensile strength of rock materials. Int J Rock Mech Min 15(3):99–103

Cai M, Kaiser PK, Suorineni F, Su K (2007) A study on the dynamic behavior of the Meuse/Haute-Marne argillite. Phys Chem Earth 32(8–14):907–916

Dai F, Xia K, Tang L (2009) Rate dependence of the flexural tensile strength of Laurentian granite. Int J Rock Mech Min. doi: 10.1016/j.ijrmms.2009.05.001

Davies ED, Hunter SC (1963) The dynamic compression testing of solids by the method of the split Hopkinson pressure bar. J Mech Phys Solids 11:155–179

Frew DJ, Forrestal MJ, Chen W (2001) A split Hopkinson pressure bar technique to determine compressive stress-strain data for rock materials. Exp Mech 41(1):40–46

Frew DJ, Forrestal MJ, Chen W (2002) Pulse shaping techniques for testing brittle materials with a split Hopkinson pressure bar. Exp Mech 42(1):93–106

Gray GT (2000) Classic split-Hopkinson pressure bar testing. ASM handbook. Mechanical testing and evaluation, vol 8. ASM Int, Materials Park, pp 462–476

Hauser FE, Simmons JA, Dorn JE, Zackay VF (1960) Response of metals to high velocity deformation. New York Interscience Pub, New York

Jiang FC, Liu RT, Zhang XX, Vecchio KS, Rohatgi A (2004) Evaluation of dynamic fracture toughness K-Id by Hopkinson pressure bar loaded instrumented Charpy impact test. Eng Fract Mech 71(3):279–287

Kolsky H (1949) An investigation of the mechanical properties of materials at very high rates of loading. Proc R Soc A Math Phys B62:676–700

Kolsky H (1953) Stress waves in solids. Clarendon Press, Oxford

Li XB, Lok TS, Zhao J, Zhao PJ (2000) Oscillation elimination in the Hopkinson bar apparatus and resultant complete dynamic stress-strain curves for rocks. Int J Rock Mech Min 37(7):1055–1060

Malinowski JZ, Klepaczko JR (1986) A unified analytic and numerical approach to specimen behavior in the split Hopkinson pressure bar. Int J Mech Sci 28(6):381–391

Meng H, Li QM (2003) Correlation between the accuracy of a SHPB test and the stress uniformity based on numerical experiments. Int J Impact Eng 28(5):537–555

Michell JH (1900) Some elementary distributions of stress in three dimensions. Proc Lond Math Soc 32:23–61

Narayanasamy R, Pandey KS (1997) Phenomenon of barrelling in aluminium solid cylinders during cold upset-forming. J Mater Process Technol 70(1–3):17–21

Nasseri MHB, Mohanty B, Robin PYF (2005) Characterization of microstructures and fracture toughness in five granitic rocks. Int J Rock Mech Min 42(3):450–460

Olsson WA (1991) The compressive strength of tuff as a function of strain rate from 10^{-6} to 10^{3}/sec. Int J Rock Mech Min Sci Geomech Abstr 28(1):115–118

Ross CA, Thompson PY, Tedesco JW (1989) Split-Hopkinson pressure-bar tests on concrete and mortar in tension and compression. ACI Mater J 86(5):475–481

Ross CA, Tedesco JW, Kuennen ST (1995) Effects of strain-rate on concrete strength. ACI Mater J 92(1):37–47

Schey JA, Venner TR, Takomana SL (1982) The effect of friction on pressure in upsetting at low diameter-to-height ratios. J Mech Work Technol 6(1):23–33

Wang QZ, Li W, Song XL (2006) A method for testing dynamic tensile strength and elastic modulus of rock materials using SHPB. Pure Appl Geophys 163:1091–1100

Xia K, Nasseri MHB, Mohanty B, Lu F, Chen R, Luo SN (2008) Effects of microstructures on dynamic compression of barre granite. Int J Rock Mech Min 45(6):879–887

Zhao J, Li HB (2000) Experimental determination of dynamic tensile properties of a granite. Int J Rock Mech Min 37(5):861–866